Mineralium Deposita (2003) 38: 727–738
DOI 10.1007/s00126-003-0364-1

ARTICLE

Karin Requia · Holly Stein · Lluís Fontboté
Massimo Chiaradia

Re–Os and Pb–Pb geochronology of the Archean Salobo iron oxide copper–gold deposit, Carajás mineral province, northern Brazil

Received: 25 April 2002 / Accepted: 18 April 2003 / Published online: 3 June 2003

Abstract Rhenium–osmium ages were determined for two molybdenite samples and a Pb–Pb age was derived from bornite–chalcopyrite–magnetite at the Salobo iron oxide copper–gold deposit to determine the timing of mineralization and its relation to the nearby Old Salobo Granite. Rhenium–osmium dating of molybdenite spatially associated with copper sulfide minerals yields ages with weighted means of 2576 ± 8 and 2562 ± 8 Ma. Removing the error multiplier introduced by the decay constant uncertainty, appropriate for comparing ages from the same isotopic system, these data convincingly argue for two temporally separated pulses of molybdenite deposition at 2576.1 ± 1.4 Ma ($n = 2$) and 2561.7 ± 3.1 Ma ($n = 3$). The 2576 ± 8 Ma age coincides with a previously published U–Pb age of 2573 ± 2 Ma for the Old Salobo Granite, suggesting that main stage ore formation may have been contemporaneous with granite magmatism. The slightly younger 2562 Ma age most likely represents new molybdenite precipitation associated with the development or reactivation of local shear zones. Lead–lead stepwise leaching of copper sulfide minerals yields a less precise isochron age of 2579 ± 71 Ma, and supports an Archean age for the Salobo ores. This is the first documentation of an Archean iron oxide copper–gold deposit, and the Re–Os and Pb–Pb geochronology herein support 2580–2550 Ma estimates for basement reactivation and regional granite magmatism associated with the development of brittle–ductile shear zones.

Keywords Archean · Iron oxide copper–gold deposit · Hydrothermal alteration · Re–Os dating

Editorial handling: L. Meinert

K. Requia (✉) · L. Fontboté · M. Chiaradia
Section des Sciences de la Terre, Université de Genève,
Rue des Maraîchers 13, 1211 Genève 4, Switzerland
E-mail: karinrequia@yahoo.com
Tel.: +41-22-7026622
Fax: +41-22-3205732

H. Stein
AIRIE Program, Department of Earth Resources,
Colorado State University, Fort Collins,
CO, 80523-1482, USA

Present address: M. Chiaradia
Center for Geochemical Mass Spectrometry,
School of Earth Sciences, University of Leeds,
Leeds LS2 9JT, UK

Introduction

The Salobo deposit is located in the Carajás mineral province, northern Brazil, which is among the world's most endowed mineralized districts (Fig. 1). Salobo was recently classified as an iron oxide copper–gold deposit (Requia and Fontboté 1999, 2000a, 2000b). This deposit occurs in Archean rocks, with reserves estimated at 789 Mt @ 0.96% Cu and 0.52 g/t Au (Souza and Vieira 2000). Previously, the iron oxide copper–gold deposit class was only recognized in Early Proterozoic to Pliocene rocks (Hitzman 2000). Among the genetic models proposed for the Salobo deposit are those suggesting a sedimentary–exhalative origin (Docegeo 1988; Lindenmayer 1990) and those consistent with a syngenetic volcanogenic model (Villas and Santos 2001). Other works suggest an origin related to the 1.8 Ga Young Salobo Granite for the deposit (Lindenmayer et al. 1995) or that the copper–gold mineralization is related to a porphyry copper system (Lindenmayer 1998). Huhn and Nascimento (1997), in their review of the Carajás copper deposits, note that certain deposits, such as Salobo and Igarapé Bahia, have similarities with iron oxide copper–gold deposits.

To test genetic models and date the mineralization, we present a Re–Os and Pb–Pb isotopic study. Our results demonstrate that the Salobo mineralization is Archean and was probably contemporaneous with granite emplacement. This first recognition of an Archean iron oxide copper–gold deposit opens Archean terranes to exploration for this deposit type.

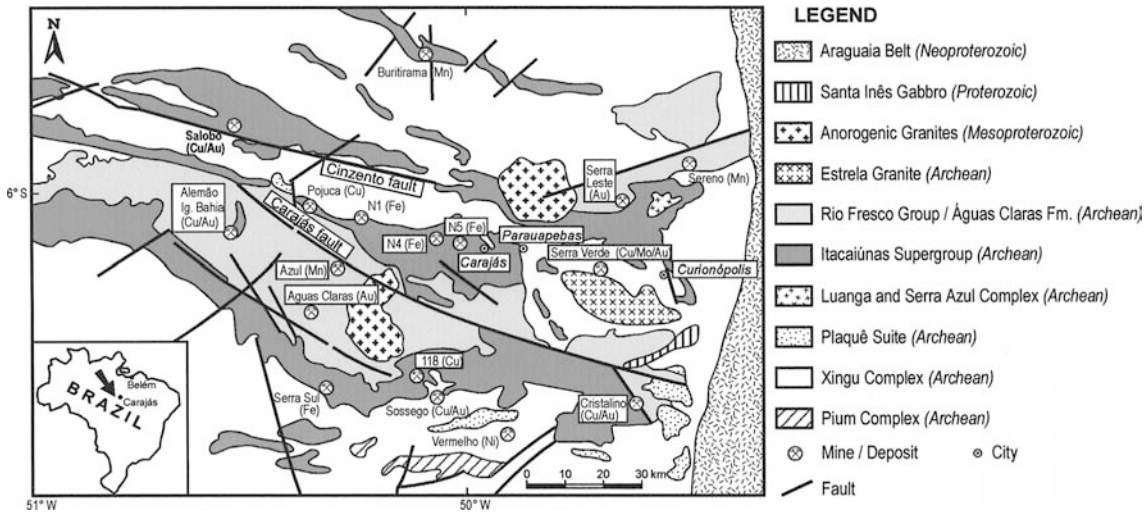

Fig. 1 Simplified geologic map of the Carajás region, including the location of principal mineral deposits (after Docegeo 1988). The Itacaiúnas Supergroup, which hosts significant ore deposits, comprises the Salobo, Pojuca, Grão-Pará, and Igarapé Bahia Groups

Regional geologic context

The Carajás mineral province lies in the southern part of the Amazonian craton, within the E–W trending Itacaiúnas shear belt (Pinheiro and Holdsworth 1997). Within this shear belt, there are two major fault systems, the Cinzento and the Carajás strike-slip systems. Both were formed during regional phases of ductile–brittle to brittle deformation and post-date the original development of the Itacaiúnas shear zone. The Cinzento strike-slip system was dated at 2.5 Ga (Pinheiro and Holdsworth 1997; Table 1), and the younger Carajás fault zone (< 1.8 Ga; Cordani 1981) is the most prominent structure in the region (Fig. 1). In addition, the Transamazonian orogeny affected the lithologies of the Carajás mineral province at about 2.2–1.8 Ga (Almeida et al. 1981).

The Xingú Complex (> 2.85 Ga; zircon U–Pb; Machado et al. 1991) and the Pium Complex (> 3.0 Ga; whole-rock Pb–Pb; Rodrigues et al. 1992) represent the continental basement of the Carajás mineral province, on which the supracrustal sequences of the Archean Itacaiúnas Supergroup were deposited (Fig. 1; Table 1). The Itacaiúnas Supergroup comprises the Salobo, Pojuca, Grão-Pará, and Igarapé Bahia Groups. It is overlain by a clastic sedimentary rock unit, the Águas Claras Formation (Araújo and Maia 1991) or Rio Fresco Group (Docegeo 1988) dated at 2681 ± 5 Ma (zircon U–Pb; Trendall et al. 1998), which is cut by 2645 ± 12 Ma (zircon Pb–Pb; Dias et al. 1996) sills and dikes of gabbro and diabase. The tectonic environment during deposition of the Itacaiúnas Supergroup was probably an extensional continental rift (Hutchinson 1979; Wirth 1986; Docegeo 1988; Lindenmayer 1990). Rocks of the resulting Carajás basin were intruded by Archean granites and diorites of the Plaquê Suite (2747 ± 2, zircon Pb–Pb, Huhn et al. 1999; 2736 ± 24 Ma, zircon Pb–Pb, Avelar et al. 1999), Estrela Complex (2763 ± 7 Ma, zircon Pb–Pb, Barros and Barbey 2000), and Old Salobo Granite (2573 ± 2 Ma, zircon U–Pb, Machado et al. 1991). Anorogenic granites of Proterozoic age (1.8–1.9 Ga, Machado et al. 1991; Cordani 1981), such as the Carajás, Cigano, Pojuca, Musa, and Young Salobo granites, also occur in the Carajás mineral province.

Deposit geology

The Salobo deposit is hosted by rocks of the Archean Salobo Group, which consist of a sequence of amphibolite, banded iron formation, metagraywacke, and quartzite (Fig. 2). This sequence ranges in thickness from at least 300 to 600 m, striking approximately N70°W, with subvertical dip. Two intrusions, the Old Salobo and Young Salobo granites, intrude rocks of the Salobo Group. The Old Salobo Granite (2573 ± 2 Ma; zircon U–Pb; Machado et al. 1991) is an alkaline, metaluminous, within-plate granite whereas the Young Salobo Granite (1880 ± 80 Ma; whole-rock Rb–Sr; Cordani 1981) is an alkaline, metaluminous, anorogenic syenite sill (Lindenmayer 1990).

The Salobo deposit is situated within the Cinzento strike-slip system, which post-dates the formation of the Itacaiúnas shear zone, and was developed under ductile–brittle to brittle conditions (Holdsworth and Pinheiro 2000; Table 1). The tectonic evolution of the Salobo area includes sinistral transpressive ductile deformation developed under upper amphibolite facies conditions, followed by sinistral transtensive ductile–brittle to brittle shear deformation (Siqueira 1996; Souza and Vieira 2000). The ductile deformation along the Itacaiúnas shear zone, which affected basement rocks and rocks of the Salobo Group, probably occurred between about 2850 and 2760 Ma (zircon U–Pb, Machado et al. 1991; Holdsworth and Pinheiro 2000; Table 1). It produced

Table 1 Main lithostratigraphic units and intrusive rocks of the Carajás mineral province (after Docegeo 1988)

Era	Age (Ma)	Methods	Complex or Supergroup	Group or Formation	Intrusive rocks	Deformation
Proterozoic	1874–1883[a,b]	U–Pb, zircon; Rb–Sr, whole rock			Anorogenic granites: Carajás, Young Salobo, Pojuca, Cigano, etc	
Archean	2552 ± 4[a]/2551 ± 2[a]	U–Pb, zircon/monazite				Cinzento strike-slip system (ductile–brittle to brittle)
	2560 ± 37[c]	Pb–Pb, zircon			Pojuca Granite	
	2573 ± 2[a]	U–Pb, zircon			Old Salobo Granite	
	2681 ± 5[d]/2645 ± 12[e]	U–Pb, zircon[4]/Pb–Pb, zircon[5]		Rio Fresco Group/Águas Claras Formation		
	2736 ± 24[f]/2747 ± 2[g]	Pb–Pb, zircon			Plaquê granitoid suite	
	*2747 ± 2[h]	Pb–Pb, zircon	Itacaiúnas Supergroup	Igarapé Bahia Group		
	*2759 ± 2[a]	U–Pb, zircon		Grão Para Group		
	*2761 ± 3[a]/2732 ± 3[a]	U–Pb, zircon		Salobo/Pojuca Groups		
	2763 ± 7[i]	Pb–Pb, zircon			Estrela granitic complex	
	*2851 ± 4[a]	U–Pb, zircon	Xingú Complex			Itacaiúnas shear zone (ductile)
	3050 ± 57[j]	Pb–Pb, whole rock	Pium Complex			

[a]Machado et al. (1991)
[b]Cordani (1981)
[c]Souza et al. (1996)
[d]Trendall et al. (1998)
[e]Dias et al. (1996)
[f]Avelar et al. (1999)
[g]Huhn et al. (1999)
[h]M.B. Macambira (perssonal communication, in Villas and Santos 2001)
[i]Barros and Barbey (2000)
[j]Rodrigues et al. (1992). See further explanations in the text
*Earliest metamorphic events determined in the Xingú Complex and Itacaiúnas Supergroup

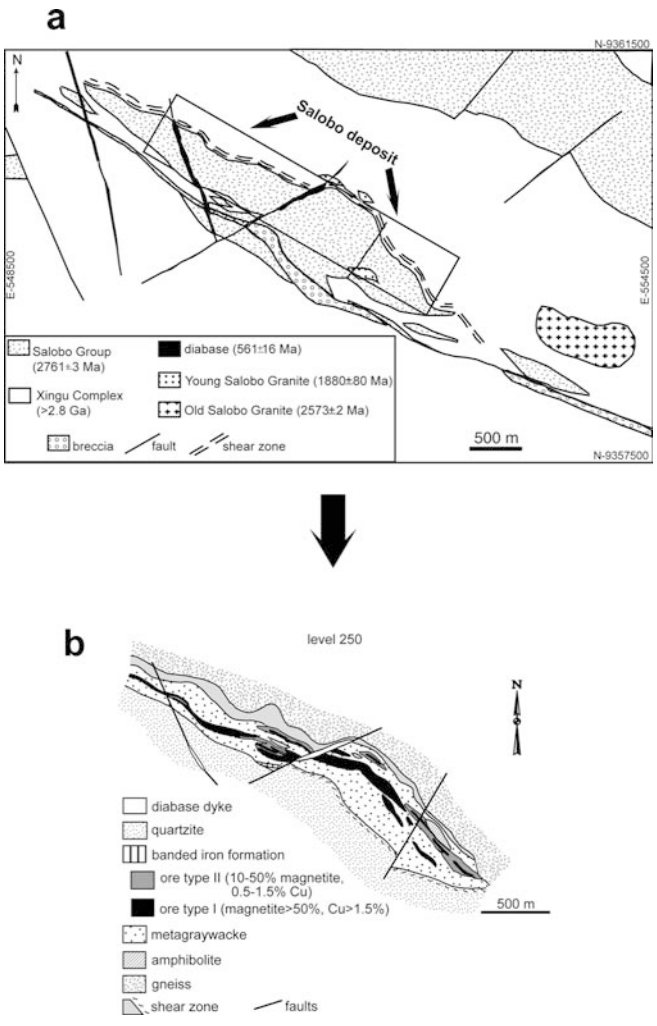

Fig. 2 **a** Simplified geologic map of the Salobo iron oxide copper–gold deposit (after Souza and Vieira 2000). The deposit is hosted by supracrustal rocks of the Archean Salobo Group, which strike approximately N70°W, with subvertical dip. **b** Deposit geology at level 250 (Docegeo 1988). At the studied area, the Salobo Group consists of a sequence of amphibolite, banded iron formation, metagraywacke, and quartzite

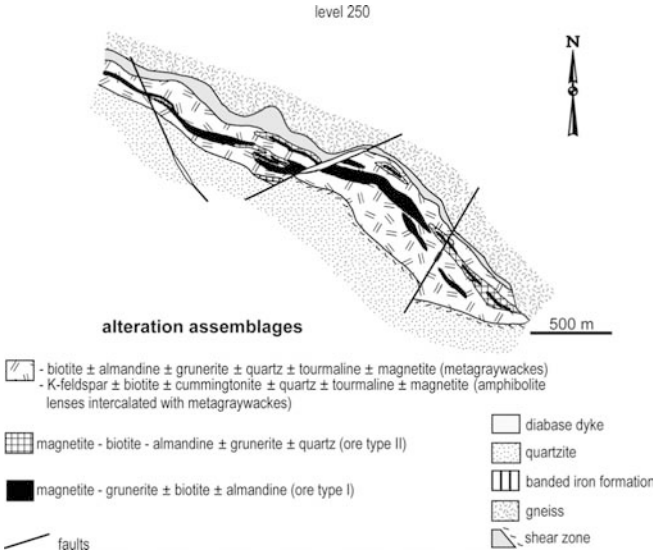

Fig. 3 Schematic distribution of hydrothermal alteration assemblages in the Salobo deposit (level 250). Dominant potassium-alteration (≤ 4.6 wt% of K_2O) is accompanied by an increase in the FeO content (≤ 35 wt%) in the amphibolite and metagraywacke host rocks. The richest ore zone, located in the central part of the deposit, corresponds to the most altered area

a widespread, subvertical, NW–SE foliation, which affects all lithologies at the deposit except the Young Salobo Granite and the diabase dikes. The transtensive deformation along the Cinzento strike-slip fault system reactivated old structures. This formed a subparallel ductile–brittle shear zone in the northern part of the deposit at about 2550 Ma (zircon/titanite U–Pb, Machado et al. 1991; Table 1), and a brittle shear zone in the south (2497 ± 5 Ma; titanite U–Pb, Machado et al. 1991).

Alteration and mineralization

Alkali-metasomatism is recognized in the amphibolite host rocks of the Salobo deposit (Requia and Fontboté 1999, 2000b). It is expressed by weak sodium alteration with intense superimposed potassium alteration (≤ 4.6 wt% of K_2O). Potassium-feldspar, biotite, and oligoclase are the main alteration minerals. A significant increase in the FeO content (≤ 35 wt%) accompanied the potassium alteration in amphibolites and was marked by the replacement of calcic-amphibole (mostly magnesium-hornblende and hastingsite) by iron–magnesium amphibole (cummingtonite), and by biotite and magnetite formation. The chemistry of the metagraywackes at the deposit reveals that they also underwent significant iron and potassium alteration (Requia 2002). Alteration assemblages are characterized by almandine garnet, biotite, and grunerite, subordinate tourmaline, and minor magnetite. The spatial distribution of hydrothermal alteration in the Salobo deposit shows that areas affected by intense iron and potassium-metasomatism host most of the iron oxide copper–gold ore (Fig. 3). The richest ore zone, located in the central part of the deposit, corresponds to the most altered area. Lindenmayer (1990) obtained a temperature of 550 °C from hydrothermal garnet rims and biotite from an ore sample in this central zone, which we interpret as representative of the thermal conditions during the iron and potassium alteration event.

The Salobo ore is characterized by large quantities of iron oxides with disseminations of chalcopyrite, bornite, and chalcocite. Magnetite is the predominant iron oxide species at Salobo. It generally forms irregular, lens-shaped, massive replacement bodies, oriented N70°W, with subvertical dip. Most of the orebodies in the deposit area are parallel to ductile–brittle shear zones, which trend NW–SE with subvertical dip, suggesting a structural control of the mineralized bodies. Two types

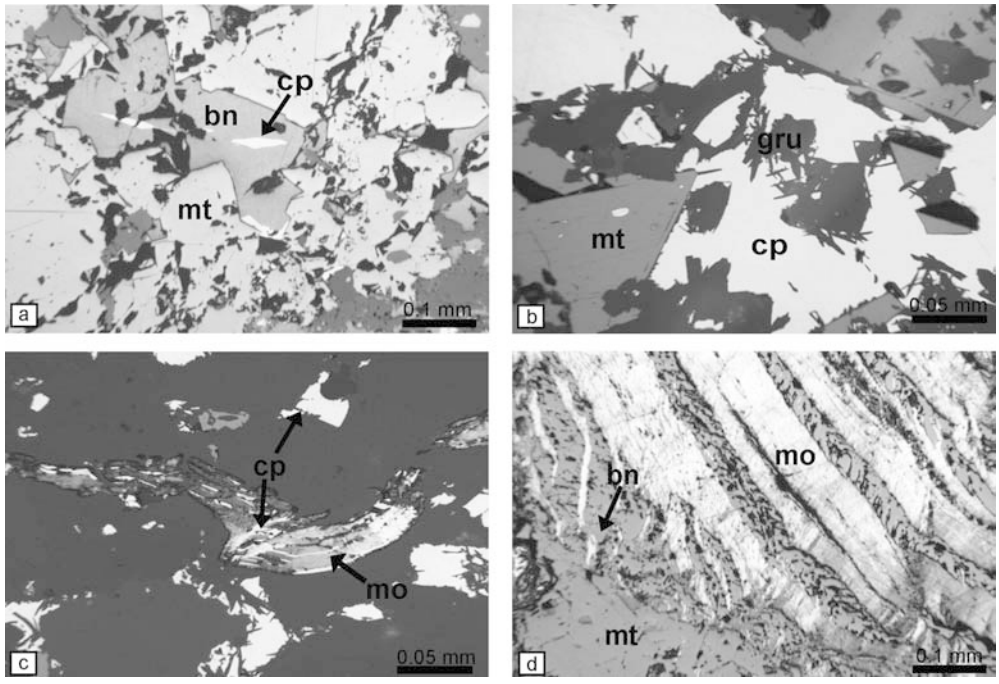

Fig. 4 Photomicrographs of ore paragenesis at the Salobo deposit (reflected light, plane polarized): **a** idiomorphic to subidiomorphic magnetite infilled by bornite and chalcopyrite, all interstitial to silicates in ore type I (KR-3); **b** chalcopyrite interstitial to magnetite and grunerite in ore type I (KRI-155); **c** chalcopyrite along cleavage planes and fractures in molybdenite in ore type I (KRI-155); **d** molybdenite vein, with subordinate bornite and magnetite, within a magnetite-rich ore type I (KRI-21-A)

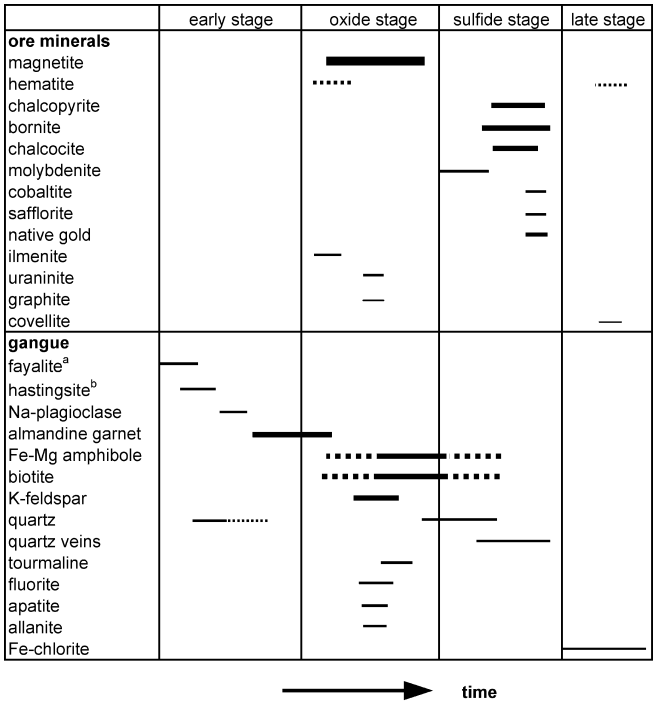

[a] pseudomorphically altered to magnetite and grunerite

[b] mostly replaced by grunerite or cummingtonite and magnetite

Fig. 5 Paragenetic sequence in the Salobo deposit

of replacement orebodies have been distinguished: ore type I (magnetite > 50%, Cu > 1.5%) and ore type II (10–50% of magnetite, 0.5–1.5% Cu). The Salobo copper–gold ore contains high Ag, As, F, Mo, U, Co, and LREE contents and low Zn, Pb, V, and Ba concentrations (Requia and Fontboté 1999, 2000b). Gold content is slightly higher in ore type I, with values up to 2 g/t relatively common.

Principal ore assemblages consist of magnetite–chalcopyrite–bornite and magnetite–bornite–chalcocite, with magnetite dominant and variable amounts of copper sulfide minerals. Accessory molybdenite is closely associated with these assemblages. In addition, quartz, fluorite, calcite, molybdenite (–bornite–magnetite), and iron-chlorite veins and veinlets occur within the iron-rich rocks. The ore minerals, in particular magnetite, replace or are interstitial to silicate assemblages. Magnetite occurs mainly as idiomorphic to subidiomorphic grains, interstitial to silicate minerals or in fractures (Fig. 4a), or forms bands interlayered with quartz–chlorite or biotite bands in mylonitic rocks. Chalcopyrite, bornite, and chalcocite occur interstitially to silicate minerals, magnetite, and hematite. These sulfide minerals are commonly found filling cleavage planes of biotite and grunerite (Fig. 4a, b). Molybdenite occurs interstitial to magnetite, in veins with subordinate bornite and magnetite, and shows cleavages planes filled with chalcopyrite and bornite (Fig. 4c, d). In mylonitic samples, molybdenite forms kinked stringers with marked variable extinction, the result of within-lath recrystallization. Hematite is rare, but in places comprises as much as 4% by volume. It exhibits tabular texture (specularite), with infilling bornite, and partial replacement by magnetite. Native gold grains are observed locally, as inclusions in cobaltite and safflorite or interstitial to bornite. In addition, ilmenite, uraninite, allanite, fluorite, and apatite occur as accessory minerals. The above textural relationships indicate that mineralization was firstly marked by an oxide stage, with a subsequent sulfide stage (Fig. 5). The oxide stage was characterized by abundant magnetite and very minor hematite. The main

sulfide stage is marked by chalcocite, bornite, and chalcopyrite formation. Petrographic evidence indicates that molybdenite formed early in the sulfide stage. Native gold precipitation appears to have occurred late in the sulfide stage, in association with cobaltite and safflorite.

Almandine garnet, grunerite, and tourmaline are the main gangue minerals reflecting the intense iron-metasomatism that affected the Salobo area. Minor amounts (< 10 vol%) of fayalite and hastingsite are pseudomorphically replaced by grunerite and magnetite. Textural features, such as almandine oriented parallel to the mylonitic foliation or rotated with small inclusions of grunerite and biotite, indicate that this mineral is associated with the deformation. Grunerite is generally subidiomorphic to idiomorphic and preferentially oriented parallel to the mylonitic foliation. Bornite and chalcocite commonly fill cleavage planes in this mineral. Tourmaline, with a dominant schorlitic composition (Requia 1995), occurs as idiomorphic crystals preferentially oriented parallel to the mylonitic foliation, in association with biotite, grunerite, and garnet. Biotite is associated with potassium-alteration and spatially related to the copper–gold ore. It occurs as subidiomorphic crystals, commonly kinked, and defines the mylonitic foliation. Cleavage planes and fractures are commonly filled by bornite and chalcocite. In addition, uraninite and zircon inclusions may be locally abundant in biotite. Quartz shows undulose extinction, and is associated with biotite in ore samples or constitutes concordant veins within the ore and host rocks.

The Salobo deposit was probably formed by high temperature, highly saline, oxidized, sulfur-poor, near-neutral pH fluids (Requia and Fontboté 2001). Total homogenization temperatures of highly saline fluid inclusions in quartz range from 173–485 °C (Requia and Xavier 1995) and geothermometry from post-ore stage chlorite yields a temperature of 350 °C (Requia et al. 1995).

Previous geochronology

Uranium–lead isotopic determinations in zircon, titanite, and monazite in rocks from the Salobo area were carried out by Machado et al. (1991). The earliest regional metamorphic event detected in the basement gneisses was dated at 2851 ± 4 Ma (zircon). At 2761 ± 3 Ma (zircon), the rocks of the Salobo Group underwent upper amphibolite facies metamorphism. Renewed basement metamorphism was observed at 2742–2732 Ma (zircon), but its significance is uncertain. According to Machado et al. (1991), a regional basement reactivation occurred in the Salobo area between about 2580 and 2550 Ma. This activity started by injection of granitic veins into the gneisses at 2581 ± 5 Ma (titanite), followed by the intrusion of the Old Salobo Granite at 2573 ± 2 Ma (zircon), and a southward thrusting of the Salobo rocks between 2573 and 2551 Ma. Zircon in mylonitized amphibolite from the Salobo deposit yielded an age of 2552 ± 4 Ma, whereas a silicified and sheared iron-rich rock from the Pojuca deposit was dated at 2551 ± 2 Ma (monazite), both indicating a period of shear zone reactivation at about 2550 Ma. A later event in the deposit area was marked by the reactivation of brittle shear zones in the south, with titanite formation in sheared amphibolite at 2497 ± 5 Ma. Clearly, the history of deformation and development, plus reactivation, of shear zones is highly complex.

Mellito and Tassinari (1998) dated chalcocite and magnetite samples from Salobo using the Pb–Pb method. Magnetite dating yielded an age of 2776 ± 240 Ma, whereas chalcocite was dated at 2762 ± 180 Ma. These authors interpret the magnetite as part of the banded iron formations and the copper ore as "syngenetic". In addition, Tassinari and Mellito (2001) performed Pb–Pb stepwise leaching on chalcopyrite, magnetite, and ore-associated tourmaline, obtaining ages of 2427 ± 130, 2112 ± 12, and 2587 ± 150 Ma, respectively. They correlate these results to regional deformation at 2.6–2.5 Ga (for chalcopyrite and tourmaline) and to the 2.2–1.8 Ga Transamazonian orogeny (for magnetite). The intrusion of the Young Salobo Granite at 1880 ± 80 Ma, and diabase dikes at 561 ± 16 Ma (whole-rock Rb–Sr, Cordani 1981) were the last igneous events in Salobo area.

Present geochronology study

Re–Os dating of molybdenite

The Re–Os chronometer is based on the beta decay of ^{187}Re (about 62% of total rhenium) to ^{187}Os. The siderophile–chalcophile nature of rhenium and osmium permit these elements to be taken directly into the sulfide mineral structure, providing a chronometer to directly date ore minerals. Molybdenite presents a unique situation for Re–Os in that it is a sink for rhenium (replacing molybdenum) and commonly has rhenium concentrations in the parts per million range. Also, molybdenite essentially excludes osmium from its structure upon formation so that common osmium concentrations are insignificant relative to time-dependent accumulation of radiogenic ^{187}Os. Because Re/Os ratios for molybdenite are extremely large, measurable radiogenic ^{187}Os accumulates after a short time and a model age can be determined from a single molybdenite sample. Geologically consistent and analytically reproducible ages for molybdenite illustrate the robustness of the chronometer (e.g., Stein et al. 1998a, 1998b; Watanabe and Stein 2000; Selby and Creaser 2001; Stein et al. 2001), even through granulite facies metamorphism (Raith and Stein 2000; Bingen and Stein 2003). This study further demonstrates that the Re–Os system in molybdenite is not disturbed by post-ore, magmatic–hydrothermal overprints.

Two molybdenite samples were selected for this study. Both samples are from a portion of a 1- to-3-cm-thick vein of molybdenite, with subordinate bornite and magnetite (Fig. 4d), taken from the exploration gallery G2 within ore type I. This vein belongs to the main orebody occurring in the central part of the deposit (Fig. 2b). In both samples, molybdenite occurs as elongate kinked laths with undulose extinction. No variations in the amounts of bornite and magnetite between the two studied samples were noted.

Repeat analyses involving different mineral separates were made on two molybdenite samples, KRI-21-A and KRI-21-B (Table 2), at the AIRIE molybdenite laboratory at Colorado State University (CSU) according to procedures outlined in Stein et al. (2001). Sample sizes for drilled molybdenite powders ranged from 10–25 mg. For this study, a Carius-tube digestion was used, whereby molybdenite is dissolved and equilibrated with ^{185}Re and ^{190}Os spikes in HNO_3–HCl (inverse aqua regia) by sealing in a thick-walled glass ampoule (Carius tube) and heating for 12 h at 230 °C. The osmium is recovered by distilling directly from the Carius tube in a manner similar to that described by Brauns (2001), except that the osmium is trapped in 5 ml of chilled HBr. The osmium is subsequently purified by micro-distillation (Birck et al. 1997). The rhenium is recovered by anion exchange (Morgan et al. 1991; Markey et al. 1998). The rhenium and osmium are loaded onto platinum filaments and isotopic compositions are determined using NTIMS on NBS 12-inch radius, 68° and 90° sector mass spectrometers at CSU. Two in-house molybdenite standards, calibrated at AIRIE, are run routinely as an internal check (Markey et al. 1998). The age is calculated by applying the equation $^{187}Os = {}^{187}Re\,(e^{\lambda t}-1)$, where λ is the decay constant for ^{187}Re and t is the age. The ^{187}Re decay constant used is 1.666×10^{-11} year^{-1}, with an uncertainty of 0.31% (Smoliar et al. 1996). Uncertainties in age calculations include error associated with (1) ^{185}Re and ^{190}Os spike calibrations, 0.05 and 0.15%, respectively, (2) weighing the spikes, (3) magnification with spiking, (4) mass spectrometric measurement of isotopic ratios, and (5) the ^{187}Re decay constant (0.31%). Molybdenites rarely require a blank correction, as is the case for Salobo. In the AIRIE molybdenite laboratory during this study, blanks were Re = < 10 pg, ^{187}Os = < 1.5 pg.

Table 2 Re–Os data for molybdenites from the Salobo iron oxide copper–gold deposit, northern Brazil. Molybdenite dissolution and spike equilibration by Carius tube. Absolute errors for concentration data in parentheses at 2σ. Ages reported at 2σ (includes all analytical and ^{187}Re decay constant uncertainties). Note that uncertainties on the weighted means are less than the ^{187}Re decay constant uncertainty of 0.31%

Sample No.	AIRIE Run	Total Re (ppm)	^{187}Os (ppb)	Age (Ma)
KR-21-A	CT-415	199.3 (1)	5493 (2)	2576 ± 8
KR-21-A	CT-423	198.4 (1)	5468 (5)	2576 ± 8
				Weighted mean = 2576 ± 6
KR-21-B	CT-424	83.17 (6)	2278 (2)	2561 ± 8
KR-21-B	CT-438	81.92 (6)	2245 (1)	2562 ± 8
KR-21-B	CT-439	80.31 (4)	2202 (1)	2563 ± 8
				Weighted mean = 2562 ± 5

Pb–Pb dating of sulfides and oxides

An acid stepwise-leaching procedure, whereby lead isotopic ratios are measured in successive leach fractions of the same mineral (Frei and Kamber 1995; Frei et al. 1997), has been successfully applied to mineral dating. This procedure is independent of element fractionation during chemical procedures applied in the laboratory, as it utilizes a single element, lead, whose relevant isotopes are decay products of the U–Pb system, and it enables Pb–Pb dating of many single minerals (e.g., Kamber et al. 1995; Frei and Pettke 1996; Kreissig et al. 2001).

In this study, we obtained lead isotope analyses on one pure bornite sample, two bornite–chalcopyrite mixtures, and three magnetite samples from both ore type I and II. In the analyzed samples, magnetite is often subidiomorphic, showing straight boundaries with copper sulfide minerals (Fig. 4a). Bornite occurs interstitial to magnetite grains (Fig. 4a), or fills cleavage planes of biotite and grunerite. This mineral commonly displays intergrowths with chalcopyrite or chalcocite, rendering it difficult to obtain concentrates of pure bornite.

The bornite–chalcopyrite mixed sulfide minerals for sample KRI-110 and the magnetite from sample KRI-48 were subjected to a stepwise-leaching procedure (Table 3) in order to recover variably radiogenic lead. Bulk fractions of bornite and bornite–chalcopyrite for samples KRI-27 and KRI-3, as well as of magnetite from samples KRI-152 and KRI-110, were also analyzed (Table 3). Stepwise leaching was carried out on 300–500 mg of powdered ore mineral (sulfide or magnetite) with 4 M HBr for different time periods (see Table 3). In total, five analyses were performed on both sulfide mineral and magnetite fractions that provided lead in sufficient amount to be measured. Because relatively large amounts of minerals were leached, common lead in these fractions was in the order of tens of nanograms. Because procedural blank lead was < 120 pg, no blank corrections of the data were necessary. Lead was purified through chromatography in hydrobromic medium using AG1-X8 and AG-MP1 resins. Lead fractions were loaded onto zone-refined single rhenium-filaments and isotope ratios were measured on a MAT Finningan 262 mass spectrometer. Lead isotope ratios were corrected for fractionation by an + 0.08% atomic mass unit correction factor based on more than 100 analyses of the NBS 981 international standard. The analytical uncertainties are 0.05% for ^{206}Pb/^{204}Pb, 0.08% for ^{207}Pb/^{204}Pb, and 0.10% for ^{208}Pb/^{204}Pb. The ^{207}Pb/^{206}Pb age was calculated using ISOPLOT software (Ludwig

Table 3 Lead–lead isotopic data for sulfides and magnetite from the Salobo iron oxide copper–gold deposit, northern Brazil. *bn* bornite, *cp* chalcopyrite, *mt* magnetite, "*r*" error correlation

Sample	Location	Ore type	Mineral	Fraction	$^{206}Pb/^{204}Pb$	2σ $^{206}Pb/^{204}Pb$	$^{207}Pb/^{204}Pb$	2σ $^{207}Pb/^{204}Pb$	$^{208}Pb/^{204}Pb$	2σ $^{208}Pb/^{204}Pb$	"r"
KRI-27	F41/407.6 m	Ore type I	bn	Bulk	294.9657	0.08	62.9162	0.08	82.9071	0.08	1.0000
KRI-3	F128/83.3 m	Ore type I	bn (67%), cp (33%)	Bulk	956.5160	0.20	181.0933	0.20	56.8437	0.19	0.9998
KRI-110	F143/703.25 m	Ore type I	bn (77%), cp (23%)	10 min 4 M HBr	25.1557	0.06	16.6731	0.06	38.2222	0.06	0.9999
KRI-110	F143/703.25 m	Ore type I	bn (77%), cp (23%)	6 h 4 M HBr	344.0979	0.06	70.1648	0.09	83.4066	0.07	0.9567
KRI-110	F143/703.25 m	Ore type I	bn (77%), cp (23%)	Residue	447.0947	0.12	88.3440	0.13	149.6163	0.11	0.9878
KRI-48-1	F48/646.25 m	Ore type I	mt	10 min 4 M HBr	99.6150	0.18	28.2116	0.20	43.2138	0.19	0.9834
KRI-48-2	F48/646.25 m	Ore type I	mt	40 min 4 M HBr	34.5695	0.63	17.9012	0.72	39.9976	0.61	0.9748
KRI-48-3	F48/646.25 m	Ore type I	mt	3 h 4 M HBr	50.1574	0.03	20.2053	0.03	41.5848	0.03	0.9972
KRI-152	F143/438.28 m	Ore type II	mt	Bulk	136.1023	0.02	32.3274	0.02	81.3517	0.02	0.9990
KRI-110	F143/703.25 m	Ore type I	mt	Bulk	76.8972	0.03	24.3075	0.04	39.4361	0.03	0.9980

2000). Age errors are reported at the 95% confidence level.

Analytical results

Re–Os analyses

Results of Re–Os analyses are shown in Table 2. Molybdenite A (KR-21-A) has a weighted mean age of 2576 ± 6 Ma ($n = 2$, 95% CL). Molybdenite B (KR-21-B) has a weighted mean age of 2562 ± 5 Ma ($n = 3$, 95% CL), and is distinctly younger than molybdenite A. These samples were initially expected to give the same age result, leading to the construction of a molybdenite ^{187}Re–^{187}Os isochron with a few replicate analyses (each replicate is a unique mineral separate), providing that a small variation in rhenium concentration was found within samples (Stein et al. 1998b). An attempt to use the isochron approach with all five samples yields a significantly negative ^{187}Os intercept in ^{187}Re–^{187}Os space, the required plotting space for molybdenites (Stein et al. 2000). This negative ^{187}Os intercept (-21.4 ± 5.7 ppb) is also a clear indication that these two samples should not be grouped together for an isochron plot, and that they represent two different populations of molybdenite deposition. This is also strongly supported by the two different and consistent rhenium concentrations associated with two molybdenite separates from sample A (200 ppm) and three separates from B (80 ppm). In addition, we checked all samples during mass spectrometry for common osmium by monitoring ^{192}Os and, as is the usual case for molybdenite, there is no measurable ^{192}Os in these two samples (Stein et al. 2001).

For any single analysis of sample A and sample B, the Re–Os ages marginally overlap at 2σ uncertainty with an absolute error of ± 8 m.y., retaining the ^{187}Re decay constant uncertainty in the comparison. If the data are first considered as a single data set of five, the resulting MSWD of 71 associated with the calculation of a weighted mean (Fig. 6) clearly indicates that the samples are not related within the confines of the assigned analytical errors. Because replicate ages for both samples are very tight and there is essentially no within-sample variation in rhenium concentration, two molybdenite-precipitating events is the simplest explanation. Isotopic disturbance does not permit tight replicate analyses from different mineral separates in a sample. Therefore, the weighted mean approach should be reapplied, but with separation of molybdenite sample A from B. The plotting of data for molybdenite A and molybdenite B (Fig. 6) indicates that there is a real temporal distinction for the formation of these two molybdenite samples. As an important technical point, comparison of Re–Os ages for different samples should remove the 0.31% uncertainty for the ^{187}Re decay constant from each analysis, as this is a constant error magnifier for all samples. Doing so, produces a weighted mean age of 2576.1 ± 1.4 Ma for molybdenite A and 2561.7 ± 3.1 Ma

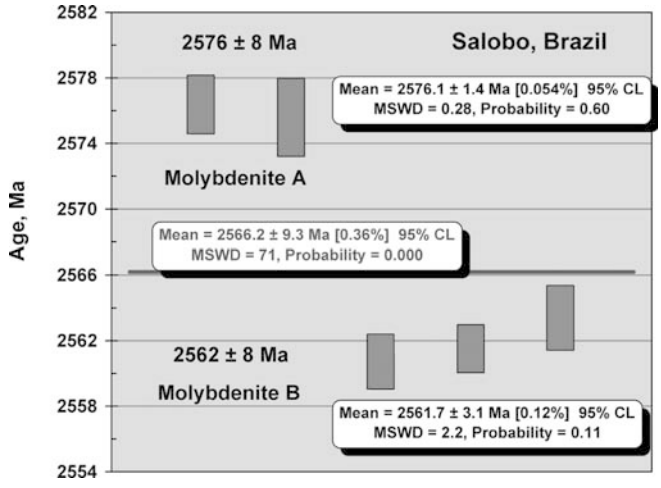

Fig. 6 Weighted means for molybdenite samples A (KRI-21-A) and B (KRI-21-B) from the Salobo iron oxide copper–gold deposit, northern Brazil. To provide the most conservative analysis of the Re–Os data, the uncertainty in the ^{187}Re decay constant, a constant error multiplier for all samples, has been removed from the five data bars, and is not included in the two resulting weighted means reported on the right side of the figure. A weighted average for all five data points yields a high MSWD of 71, supporting two populations of analytical results. When comparing Re–Os results with ages from other isotopic methods, the error for the Re–Os weighted mean ages should be reported as ±8 Ma to include the uncertainty in the decay constant. Analytical data are in Table 2. Text offers additional explanation

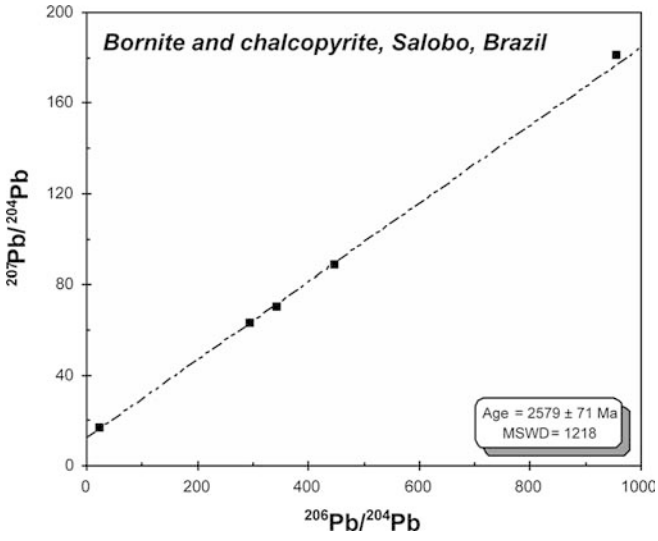

Fig. 7 ^{207}Pb/^{204}Pb vs. ^{206}Pb/^{204}Pb correlation diagram and age for copper sulfide minerals from the Salobo deposit using the model 1 of Ludwig (2000). Data point symbols exceed dimensions of error bars

for molybdenite B (Fig. 6). The uncertainty on both of these ages is markedly reduced, because the data are in remarkably good agreement for replicates of each sample. It is important that, for comparison with radiometric ages obtained by other isotopic methods, an uncertainty of ±8 Ma for the weighted mean age be used, so that the errors on the weighted mean Re–Os ages include the uncertainty in the ^{187}Re decay constant (Stein et al. 2001). Therefore, the Re–Os ages that should be quoted for Salobo molybdenites, and used when comparing Re–Os ages with other ages by other methods, are 2576 ± 8 Ma for molybdenite A and 2562 ± 8 Ma for molybdenite B. Unfortunately, errors in published U–Pb ages almost always exclude the decay constant uncertainty for parental isotopes of uranium. Thus, reported errors for U–Pb ages are unrealistically small when drawing comparisons with other isotopic systems, such as Re–Os.

Pb–Pb analyses

The precision and accuracy that is offered by Re–Os dating of molybdenites provides a fixed point to test the accuracy of the Pb–Pb method applied to sulfide minerals and magnetite from the Salobo deposit. Lead–lead ages of sulfide minerals are based on three stepwise-leached fractions of a single sample (KRI-110) plus two analyses on bulk bornite fractions (Table 3). A five-point isochron yields an age of 2579 ± 71 Ma (model 1, Ludwig 2000; Fig. 7). Recalculation of the age based on equal weights and zero error-correlations (model 2, Ludwig 2000) provides an age of 2626 ± 70 Ma.

The ^{206}Pb/^{204}Pb values obtained on stepwise-leached magnetite fractions of sample KRI-48 and on bulk magnetite (samples KRI-152 and KRI-110) are significantly lower than those of the sulfide minerals, suggesting lower μ (^{238}U/^{204}Pb) values in magnetite compared to sulfides. An isochron based on the regression of five points (three stepwise-leached fractions and two bulk fractions) yields ages of 2291 ± 220 and 2297 ± 240 Ma, respectively, for models 1 and 2.

Discussion

Re–Os results

We suggest that ages for both molybdenite A and B provide significant information that is integral to understanding the larger geologic and ore-forming history at Salobo. The weighted mean age of 2576 ± 6 Ma for molybdenite A is in good agreement with the 2573 ± 2 Ma U–Pb age for the Old Salobo Granite obtained by Machado et al. (1991). Based on the geologic and geochronologic data, we suggest that molybdenite A is related to main stage ore deposition and that this event is contemporaneous to intrusion of the Old Salobo Granite.

Although some authors suggest that the Re–Os chronometer could be isotopically disturbed (Suzuki et al. 2000, 2001), the reproducible difference in the ages for these two molybdenite samples does not support a scenario of "isotopic disturbance" for molybdenite A or B as an explanation for the different ages. We suggest that this younger age is associated with the deposition of

new molybdenite at ~2562 Ma, possibly in association with the development (or reactivation) of shear zones at Salobo. In a similar study involving Late Archean granitoids and a porphyry Cu–Mo system at Malanjkhand, India, Re–Os ages in molybdenite also record several overprinting episodes of Early Proterozoic deformation in the ore system, reflecting development of the Central Indian tectonic zone (Hannah et al. 2002).

An alternative explanation for Salobo molybdenite A is that the 2576 ± 6 Ma age may reflect molybdenite deposition associated with the development of older shear zones affecting the deposit, with main stage ore deposition older than and unrelated to the Old Salobo Granite. However, the full geologic and geochronologic evidence best supports an initial period of granite-related mineralization, followed by deformation and redistribution of some ore components.

Pb–Pb results

The 2579 ± 71 Ma Pb–Pb age of sulfide minerals, despite a larger error, is the same as the Re–Os ages of molybdenites. The high MSWD for this isochron documents scatter beyond the assigned analytical uncertainty for the data points. This excess scatter is most likely geologic, either from variation in the initial ratio for samples, or from small degrees of open system behavior. For cases where it is evident that some other cause of scatter is involved, recalculation of the age based on equal weights and zero error-correlations may be used (model 2, Ludwig 2000). This calculation yields an age of 2626 ± 70 Ma, the same within error as that obtained using model 1. Although the U–Pb system in the analyzed sulfide minerals was potentially disturbed by later geologic processes, the less precise Pb–Pb ages are consistent with the Re–Os molybdenite ages. Lead–lead dating of magnetite (2291 ± 220 Ma) also shows a high MSWD value (556) associated with this isochron, indicating excess scatter and possibly open system behavior. The magnetite age is the same, within error, as those from the sulfide minerals, but open system behavior seems to have more significantly affected the magnetite fractions than the sulfides.

Also the imprecise and geologically variable Pb–Pb ages obtained by Mellito and Tassinari (1998) and Tassinari and Mellito (2001) on chalcocite, magnetite, chalcopyrite, and ore-associated tourmaline from the Salobo deposit (2776 ± 240, 2762 ± 180, 2427 ± 130, and 2587 ± 150 Ma, respectively), confirm the difficulties in the application of Pb–Pb dating to the Salobo minerals. Nevertheless, despite the large uncertainties, these determinations are compatible with an Archean age for the mineralization.

In conclusion, Pb–Pb dating of sulfide minerals from the Salobo iron oxide copper–gold deposit yields more accurate and precise ages than magnetite dating. Our bornite–chalcopyrite five-point isochron yielding an age of 2579 ± 71 Ma is consistent with the Re–Os age determinations of 2576 ± 8 and 2562 ± 8 Ma. However, we note that, in the absence of Re–Os ages, the Pb–Pb age, although geologically meaningful, would be of limited value in resolving temporal differences in the geologic and ore-forming history because of its high MSWD and large 2σ uncertainty.

Metallogenetic implications

The new age determinations in this study support existing geometric relationships and geochemical data (e.g., Requia and Fontboté 1999, 2000a, 2000b, 2001), which suggest Salobo is an iron oxide copper–gold deposit of Archean age formed near the ductile–brittle transition and of probable magmatic affiliation. The geochronological data do not support a genetic relationship between the Salobo ore and the anorogenic Young Salobo Granite (1880 ± 80 Ma; whole-rock Rb–Sr, Cordani 1981), as proposed by Lindenmayer et al. (1995). Also, the sedimentary–exhalative and other syngenetic models, assumed by some authors (Docegeo 1988; Lindenmayer 1990; Villas and Santos 2001), are not compatible with the age determinations in this study.

Regional chronologic relationships are summarized in Fig. 8. At least two temporally distinct molybdenite events (Fig. 8) are strongly supported by the different rhenium concentrations (Table 2). It is unlikely that a single molybdenite-depositing, high temperature fluid would produce contemporaneous molybdenites with 80 and 200 ppm Re in the same vein at the same location. We suggest main stage copper–gold deposition occurred at 2576 ± 8 Ma, contemporaneous with nearby granite magmatism. Additional molybdenite

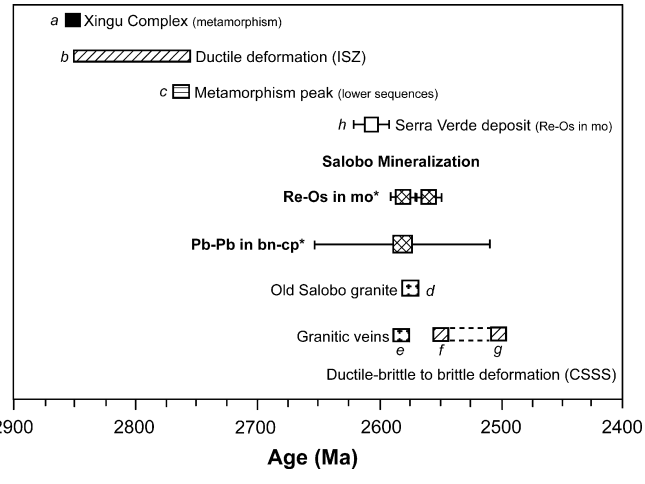

Fig. 8 Summary of regional chronologic relationships. Data after Machado et al. (1991): *a* 2851 ± 4 Ma; *b* 2851–2761 Ma; *c* 2761 ± 3 Ma; *d* 2573 ± 2 Ma; *e* 2581 ± 5 Ma; *f* 2552 ± 4 and 1551 ± 2 Ma; *g* 2497 ± 5 Ma; and Marschik et al (2001): *h* 2609 ± 13 Ma. *ISZ* Itacaiúnas Shear Zone, *CSSS* Cinzento strike-slip system; *bn* bornite; *cp* chalcopyrite; *mo* molybdenite; * data from this study. See further explanation in the text

precipitation occurred at 2562 ± 8 Ma and was probably related to reactivation (or development) of local shear zones. An alternative possibility is that 2576 ± 8 Ma molybdenite deposition corresponds to older shear zone development in the Salobo area, and is unconnected to magmatism of this age. However, geologic and geochemical considerations do not favor this alternative explanation (Requia and Fontboté 1999, 2000a, 2000b).

A distinctly older Re–Os age of 2609 ± 13 Ma was determined for molybdenite from the Serra Verde copper–molybdenum–gold deposit (Marschik et al. 2001; Fig. 8), located near the Archean Estrela Granitic Complex (2763 ± 7 Ma, zircon Pb–Pb, Barros and Barbey 2000; Fig. 1). Disturbed $^{40}Ar/^{39}Ar$ spectra of amphibole spatially associated with the ore in the Sossego iron oxide copper–gold deposit, located in the southern part of the Carajás basin (Fig. 1), suggest a minimum alteration age of 2.2–2.3 Ga (Marschik and Leveille 2001).

Conclusions

Rhenium–osmium dating of two molybdenite samples spatially associated with copper sulfide minerals yields two ages with weighted means of 2576 ± 8 Ma and 2562 ± 8 Ma at the Salobo iron oxide copper–gold deposit. Removing the error multiplier associated with the ^{187}Re decay constant, appropriate for comparing ages derived from the same isotopic system, provides two significantly different times of molybdenite deposition, at 2576.1 ± 1.4 Ma ($n = 2$) and 2561.7 ± 3.1 Ma ($n = 3$). Lead–lead stepwise leaching of copper sulfide minerals yields a less precise age of 2579 ± 71 Ma, which is the same, within error, as those obtained with the Re–Os dating. The Re–Os age of 2576 ± 8 Ma is in good agreement with the 2573 ± 2 Ma U–Pb age for the Old Salobo Granite, thus precluding an association between mineralization and the Proterozoic Young Salobo Granite. The younger 2562 ± 8 Ma molybdenite age probably reflects development and/or reactivation of local shear zones affecting the Salobo deposit. We regard the agreement in Re–Os and U–Pb ages for molybdenite and zircon from the Old Salobo Granite, together with existing field and geochemical data, as strong evidence for a magmatic-related origin for the Salobo mineralization. The Re–Os and U–Pb geochronology at Salobo documents the first iron oxide copper–gold deposit of Archean age.

Acknowledgements We are grateful to G. Brown and N. Grant from Anglo-American Plc for financing the initial Re–Os analyses of the two molybdenite samples. We also appreciate the CVRD's logistic support during the field campaign. Richard Markey, AIRIE-Colorado State University, provided the Re–Os analyses. This work was supported by a Swiss SNF grant and was supplemented by funds from NSF EAR-0087483 (Stein) for added replicate analyses needed to establish the separation of ages for the two molybdenites. Journal reviewers David Selby and Pat Williams, as well as Richard Goldfarb, provided insightful and helpful comments.

References

Almeida F, Hasui I, Brito Neves BB, Fuck RA (1981) Brazilian structural provinces. Earth Sci Rev 17:1–29

Araújo OJB, Maia RGN (1991) Programa Grande Carajás, Serra dos Carajás, Folha SB.22-Z-A, Estado do Pará. DNPM/CPRM, Brasília

Avelar VG, Lafon JM, Correia FCJr, Macambira EMB (1999) O magmatismo arqueano da regiao de Tucuma, Provincia Mineral de Carajás, Amazônia Oriental, Brasil: novos dados geocronologicos. Rev Bras Geociê 29:453–460

Barros CEM, Barbey, P (2000) Significance of garnet-bearing metamorphic rocks in the Archean supracrustal series of the Carajás Mining Province, northern Brazil. International Congress of Geology, Rio de Janeiro, vol 31, part 3, pp 367–370

Bingen B, Stein H (2003) Granulite facies biotite dehydration melting determined by the Re–Os dating of molybdenite, Rogaland, S. Norway. Earth Planet Sci Lett (in press)

Birck JL, Barman MR, Capmas F (1997) Re–Os isotopic measurements at the femtomole level in natural samples. Geostand Newsl 20(1):19–27

Brauns CM (2001) A rapid, low-blank technique for the extraction of osmium from geological samples. Chem Geol 176:379–384

Cordani U (1981) Comentários sobre as determinações geocronológicas da região da Serra dos Carajás. Report,Universidade de São Paulo-Docegeo

Dias GS, Macambira MJB, Dall'Agnol R, Soares ADV, Barros CEM (1996) Datação de zircões de sill de metagabro: comprovação da idade arqueana da Formação Águas Claras, Carajás, Pará. Simpósio de Geologia da Amazonia, 5, Extended Abstracts, Belém, SBG, pp 376–379

Docegeo (1988) Revisão litoestratigráfica da Província Mineral de Carajás. Congr Brasileiro de Geologia, 35, Belém. SBG, Anexo aos anais, pp 11–54

Frei R, Kamber BS (1995) Single mineral Pb–Pb dating. Earth Planet Sci Lett 129:261–268

Frei R, Pettke T (1996) Mono-sample Pb–Pb dating of pyrrhotite and tourmaline: Proterozoic vs. Archean gold mineralization in Zimbabwe. Geology 24:823–826

Frei R, Villa IM, Nagler TF, Kramers JD, Przybylowicz WJ, Prozesky VM, Hofmann BA, Kamber BS (1997) Single mineral dating by Pb–Pb step leaching method: assessing the mechanisms. Geochim Cosmochim Acta 61: 393–414

Hannah J, Stein H, Zimmerman A, Markey R, Sarkar SC, Pal AB (2002) Late Archean–Early Proterozoic formation and reworking of a porphyry Cu(Mo) deposit recorded in molybdenite: Re–Os dating at Malanjkhand, central India. Geochim Cosmochim Acta 66(15A):A308

Hitzman MW (2000) Iron oxide–Cu–Au deposits: what, where, when and why. In: Porter TM (ed) Hydrothermal iron oxide copper–gold and related deposits: a global perspective. Australian Mineral Foundation, Adelaide, pp 9–26

Holdsworth R, Pinheiro R (2000) The anatomy of shallow-crustal transpressional structures: insights from the Archean Carajás fault zone, Amazon, Brazil. J Struct Geol 22:1105–1123

Huhn SRB, Nascimento JAS (1997) São os depósitos cupríferos de Carajás do tipo Cu–Au–U–ETR? In: Costa ML, Angelica RS (coord) Contribuicões à Geologia da Amazonia, SBG, Belém, pp 142–160

Huhn SRB, Macambira MJB, Dall'Agnol R (1999) Geologia and geochronologia Pb–Pb do granito alcalino Planalto, região da Serra do Rabo, Carajás, PA. Simpósio de Geologia da Amazônia, 6, Manaus, pp 463–466

Hutchinson RW (1979) Trace element mobility during hydrothermal alteration of oceanic basalts. Geochim Cosmochim Acta 42:127–136

Kamber BS, Blenkinsop TG, Villa IM, Dahl PS (1995) Proterozoic transpressive deformation in the Northern Marginal Zone, Limpopo Belt, Zimbabwe. J Geol 103:493–508

Kreissig K, Holzer L, Frei R, Villa IM, Kramers JD, Kroner A, Smit CA, van Reenen DD (2001) Geochronology of the Hout River Shear Zone and the metamorphism in the Southern Marginal Zone of the Limpopo Belt, Southern Africa. Precambrian Res 109:145–173

Lindenmayer ZG (1990) Salobo Sequence, Carajás, Brazil: geology, geochemistry and metamorphism. PhD Thesis, University of Western Ontario

Lindenmayer Z (1998) O depósito de Cu (Au–Ag–Mo) do Salobo, Serra dos Carajás, Revisitado.Workshop Depósitos Minerais Brasileiros de Metais-Base. ADIMB-CPGG-UFBA-CAPES-PADCT, Salvador, Bahia, pp 29–37

Lindenmayer ZG, Laux JH, Viero AC (1995) O papel da alteração hidrotermal nas rochas da Bacia Carajás. Bol Mus Paraense Emilio Goeldi, Sér Ciênc Terra 7:125–145

Ludwig KR (2000) User's manual for ISOPLOT/EX version 2.2: a geochronological toolkit for Microsoft Excel. Berkeley Geochronology Center, Spec Publ no 1a

Machado N, Lindenmayer Z, Krogh TE, Lindenmayer D (1991) U–Pb geochronology of Archean magmatism and basement reactivation in the Carajás area, Amazon shield, Brazil. Precambrian Res 49:239–354

Markey RJ, Stein HJ, Morgan JW (1998) Highly precise Re–Os dating of molybdenite using alkaline fusion and NTIMS. Talanta 45:935–946

Marschik R, Leveille R (2001) Iron oxide Cu–Au deposits in South America: Candelaria, Chile, and Sossego, Brazil. GSA Annual Meeting, Boston, Abstracts with programs 33(6), p A-2

Marschik R, Mathur R, Spangenberg JE, Ruiz J, Leveille R, De Almeida AJ (2001) The Serra Verde Cu–Mo–Au deposit, Carajás Mineral Province, Pará state, Brazil. GSA Annual Meeting, Boston, Abstracts with programs 33(6), p A-418

Mellito KM, Tassinari C (1998) Aplicaçao dos métodos Rb–Sr e Pb–Pb à evoluçao da mineralizaçao cuprifera do deposito de Salobo 3 A, Provincia Mineral de Carajas, PA. Congresso Brasileiro de Geologia, 40, Proceedings, Belo Horizonte, SBG, p 119

Morgan JW, Golightly DW, Dorzapf AF Jr (1991) Methods for the separation of rhenium, osmium, and molybdenum applicable to isotope geochemistry. Talanta 38:259–265

Pinheiro RVL, Holdsworth RE (1997) Reactivation of Archean strike-slip fault systems, Amazon region, Brazil. J Geol Soc Lond 154:99–103

Raith JG, Stein HJ (2000) Re–Os dating and sulfur isotope composition of molybdenite from tungsten deposits in western Namaqualand, South Africa: implications for ore genesis and the timing of metamorphism. Miner Deposita 35:741–753

Requia K (1995) O papel do metamorfismo e fases fluidas na gênese da mineralização de cobre de Salobo, Província Mineral de Carajás, Pará. MSc Thesis, Universidade Estadual de Campinas, São Paulo

Requia K (2002) The Archean Salobo iron oxide copper–gold deposit, Carajás Mineral Province, Brazil. PhD Thesis, University of Geneva

Requia K, Fontboté L (1999) Hydrothermal alkali-metasomatism in the host amphibolites of the Salobo iron oxide Cu (–Au) deposit, Carajás Mineral Province, northern Brazil. In: Stanley CJ et al. (eds) Mineral deposits: processes to processing. Balkema, Rotterdam, pp 1025–1028

Requia K, Fontboté L (2000a) The Salobo iron oxide Cu (–Au) deposit, Carajás Mineral Province, northern Brazil: evidences of hydrothermal alkali-metasomatism in the host amphibolites. International Geological Congress, 31, Rio de Janeiro, Brazil. Abstracts, CD-ROM, 1 p

Requia K, Fontboté L (2000b) The Salobo iron oxide copper-gold deposit, Carajás, northern Brazil. In: Porter TM (ed) Hydrothermal iron oxide copper–gold and related deposits: a global perspective. Australian Mineral Foundation, Adelaide, pp 225–236

Requia K, Fontboté L (2001) The Salobo iron oxide copper–gold hydrothermal system, Carajás Mineral Province, Brazil. GSA Annual Meeting, Boston, Abstracts with programs, 33(6), p A-2

Requia K, Xavier RP (1995) Fases fluidas na evolução metamórfica do depósito polimetálico de Salobo, Província Mineral de Carajás, Pará. Rev Escola Minas, Ouro Preto, 49(2):117–122

Requia K, Xavier RP, Figueiredo B (1995) Evolução paragenética, textural e das fases fluidas no depósito polimetálico de Salobo, Província Mineral de Carajás, Pará. Bol Mus Paraense Emilio Goeldi, Sér Ciênc Terra 7:27–39

Rodrigues ES, Lafon JM, Scheller T (1992) Geocronologia Pb–Pb da Província Mineral de Carajás: primeiros resultados. Congresso Brasileiro de Geologia, 37, São Paulo. SBG, Resumos expandidos 2, pp 183–184

Selby D, Creaser RA (2001) Re–Os geochronology and systematics in molybdenite from the Endako porphyry molybdenum deposit, British Columbia, Canada. Econ Geol 96:197–204

Siqueira JB (1996) Aspectos litoestruturais e mineralizações do depósito Salobo 3A, Serra dos Carajás, Pará. PhD Thesis, Federal University of Pará, Brazil

Smoliar MI, Walker RJ, Morgan JW (1996) Re–Os isotope constraints on the age of Group IIA, IIIA, IVA, and IVB iron meteorites. Science 271:1099–1102

Stein HJ, Morgan JW, Markey RJ, Hannah JL (1998a) An introduction to Re–Os: what's in it for the mineral industry? SEG Newsl 32(1):8–15

Stein HJ, Sundblad K, Markey RJ, Morgan JW, Motuza G (1998b) Re–Os ages for Archean molybdenite and pyrite, Kuittila-Kivisuo, Finland and Proterozoic molybdenite, Kabeliai, Lithuania: testing the chronometer in a metamorphic and metasomatic setting. Miner Deposita 33:329–345

Stein HJ, Morgan JW, Scherstén A (2000) Re–Os dating of low-level highly-radiogenic (LLHR) sulfides: the Harnäs gold deposit, southwest Sweden records continental scale tectonic events. Econ Geol 95:1657–1671

Stein HJ, Markey RJ, Morgan JW, Hannah JL, Scherstén A (2001) The remarkable Re–Os chronometer in molybdenite: how and why it works. Terra Nova 13(6): 479–486

Souza LJ, Vieira EA (2000) Salobo 3 Alpha deposit: geology and mineralization. In: Porter TM (ed) Hydrothermal iron oxide copper–gold and related deposits: a global perspective. Australian Mineral Foundation, Adelaide, pp 213–224

Souza SRB, Macambira MJB, Scheller T (1996) Novos dados geocronológicos para os granites deformados do Rio Itacaiúnas (Serra dos Carajás, PA): implicações estratigráficas. Simpósio de Geologia da Amazônia, 5, Belém, Boletim de Resumos Expandidos pp 380–383

Suzuki K, Kagi H, Nara M, Takano B, Nozaki Y (2000) Experimental alteration of molybdenite: evaluation of the Re–Os system, infrared spectroscopic profile and polytype. Geochim Cosmochim Acta 64:223–232

Suzuki K, Feely M, O'Reilly C (2001) Disturbance of the Re–Os chronometer of molybdenites from the late-Caledonian Galway granite, Ireland, by hydrothermal fluid circulation. Geochem J 35:29–35

Tassinari CCG, Mellito K (2001) Evidências isotópicas de Sr, Pb e Nd de fontes continentais para os fluidos das mineralizações do depósito de Cu (Au, Mo, Ag) Salobo 3-A, Serra dos Carajás, Brasil. Congresso de Geoquimica dos Países de Língua Portuguesa, 6, Faro, Portugal, Actas, pp 201–204

Trendall AF, Basei MAS, De Laeter JR, Nelson DR (1998) SHRIMP zircon U–Pb constraints on the age of the Carajás formation, Grão Pará Group, Amazon craton. J S Am Earth Sci 11:265–277

Villas RN, Santos MD (2001) Gold deposits of the Carajás Mineral Province: deposit types and metallogenesis. Miner Deposita 36:300–331

Watanabe Y, Stein HJ (2000) Re–Os ages for the Erdenet and Tsagaan Suvarga porphyry Cu–Mo deposits, Mongolia, and tectonic implications. Econ Geol 95(7):1537–1542

Wirth KR (1986) The geology and geochemistry of the Grão Pará Group, Serra dos Carajás, Pará, Brazil. MSc Thesis, Cornell University, Ithaca, New York